Final state interactions and CP violation in $B^\pm \to \pi^\pm\pi^\mp\pi^\pm$ decays

J.-P. Dedonder,[1] A. Furman,[2] R. Kamiński,[3] L. Leśniak,[3] and B. Loiseau[1]

[1]*Laboratoire de Physique Nucléaire et de Hautes Énergies, Groupe Théorie, Université Pierre et Marie Curie et Université Paris-Diderot, IN2P3 & CNRS, 4 place Jussieu, 75252 Paris, France*

[2]*ul. Bronowicka 85/26, 30-091 Kraków, Poland*

[3]*Division of Theoretical Physics, The Henryk Niewodniczański Institute of Nuclear Physics, Polish Academy of Sciences, 31-342 Kraków, Poland*

(Dated: November 4, 2010)

Abstract

We study CP violation and the contribution of the strong pion-pion interactions in the three-body $B^\pm \to \pi^\pm\pi^\mp\pi^\pm$ decays within a quasi two-body QCD factorization approach. The short distance interaction amplitude is calculated in the next-to-leading order in the strong coupling constant with vertex and penguin corrections. The meson-meson final state interactions are described by pion non-strange scalar and vector form factors. The pion scalar form factor is calculated from a unitary relativistic coupled-channel model including $\pi\pi$, $K\bar{K}$ and effective $(2\pi)(2\pi)$ interactions. The pion vector form factor results from a Belle Collaboration analysis of $\tau^- \to \pi^-\pi^0\nu_\tau$ data. The recent $B^\pm \to \pi^\pm\pi^\mp\pi^\pm$ BABAR Collaboration data are fitted with our model using only three parameters for the S wave and one for the P wave. We find not only a sizable contribution of the S wave above the $\pi\pi$ threshold and near 1.4 GeV but also a significant interference between the S and P waves. Our model yields a unified unitary description of the contribution of the three scalar resonances $f_0(600)$, $f_0(980)$ and $f_0(1400)$ in terms of the pion non-strange scalar form factor.

PACS numbers: 13.25.Hw, 13.75Lb

I. INTRODUCTION

Three-body charmless hadronic B meson decays offer one of the best tools for studies of direct CP violation and provide an interesting testing ground for strong interaction dynamical models. The present work, part of a program devoted to the understanding of rare three-body B decays [1–4], is motivated by the recent BABAR Dalitz-plot analysis of the $B^\pm \to \pi^\pm\pi^\mp\pi^\pm$ decays [5]. In an isobar model description, the authors of ref. [5] find evidence for the $f_0(1370)$ but, within the current experimental accuracy, no significant signal for the $f_0(980)$. The $f_0(600)$, not explicitly included in that analysis, could be part of the non-resonant background.

Here, the aim is to provide a phenomenological analysis of the $B^\pm \to \pi^\pm\pi^\mp\pi^\pm$ decay channels relying on the QCD factorization scheme (QCDF) in the $\pi\pi$ effective mass range from threshold to 1.64 GeV. The focus will be set on the final state $\pi\pi$ interactions involved since a partial wave analysis of the Dalitz plot should use theoretically and phenomenologically well constrained $\pi\pi$ amplitudes.

Studies of B decays into two-body and quasi-two-body final states have been performed in the QCDF framework [6–12]. The naive factorization approach is a useful first order approximation which receives corrections proportional to the strong coupling constant α_s at scales m_b and $\sqrt{\Lambda_{QCD} m_b}$ and in inverse powers of the b quark mass m_b [13]. In the present study, we propose an extension of these results to a class of three-body decays $B^\pm \to \pi^\pm\ \pi^+\pi^-$.

The role of the $f_0(600)$ (or σ) in charmless three-body decays of B mesons has been examined by Gardner and Meißner [8] in $B^0 \to \pi^+\pi^-\pi^0$ decays. Within a QCD quasi two-body factorization approach their $f_0(600)\pi$ amplitude is described by a unitary pion scalar form factor constrained by $\pi\pi$ scattering and chiral dynamics, a different approach compared to the relativistic Breit-Wigner expressions used in most experimental and in some theoretical analyses, for example in [14]. This has led to improved theoretical predictions; these authors have found that the contribution of the $f_0(600)\pi$ channel was important in the range of the dominant $\rho^0\pi^0$ intermediate state. However, in recent $B^0 \to \pi^+\pi^-\pi^0$ Dalitz plot analyses [15, 16] no contribution from $B^0 \to f_0(600)\pi^0$ channel has been found. This could be linked to the present limited statistics in the low effective $\pi\pi$ mass region. Furthermore, such a contribution could be hidden in the nonresonant amplitude introduced in the experimental analysis. Nevertheless we will show that the contribution of the S wave is important in the $B^\pm \to \pi^\pm\ \pi^+\pi^-$ decays.

Charmless three-body decays of B mesons have also been investigated by Cheng, Chua and Soni [12] in the framework of quasi two-body factorization approach using resonant and non-

resonant contributions. In particular they have calculated the $B^- \to \pi^+\pi^-\pi^-$ branching fractions and CP asymmetries and found a small rate for $B^- \to f_0(980)\pi^-$decay. An achievement in the theory of B decays into two mesons is the confirmation of the validity of factorization as a leading order approximation. No proof of factorization has yet been given for the B decays into three mesons. However, three-body interactions are suppressed when specific kinematical configurations with the three mesons quasi aligned in the rest frame of the B meson are considered. This is the case in the effective $\pi^+\pi^-$ mass region smaller than 1.64 GeV in the Dalitz plot where most of the $\pi^+\pi^-$ resonant states are visible. Such processes will be denoted as $B^\pm \to \pi^\pm[\pi^+\pi^-]$, the mesons of the $[\pi^+\pi^-]$ pair moving more or less, in the same direction in the B rest frame. Then, it seems reasonable to postulate the validity of factorization for this quasi two-body B decay [17] assuming furthermore that the $[\pi^+\pi^-]$ pair originates from a quark-antiquark state.

In the factorization approach the $B^\pm \to \pi_1^\pm\ [\pi_2^+\pi_3^-]$ decay amplitudes are expressed as a superposition of appropriate effective QCD coefficients and two products of two transition matrix elements. The transition matrix elements between the $B^\pm$ meson and the $\pi_1^\pm$ pion multiplied by the transition matrix elements between the vacuum and the $\left[\pi_2^+\pi_3^-\right]$ pion pair correspond to the first of these products. The second is associated to the product of the transition matrix elements between the $B^\pm$ meson and the $[\pi_2^+\pi_3^-]$ pion pair by the transition matrix elements between the vacuum and the $\pi_1^\pm$ pion. In the $\pi_2^+\pi_3^-$ center of mass frame, the bilinear quark currents involved force the $[\pi_2^+\pi_3^-]$ pair to be in S or in P state. The $[\pi_2^+\pi_3^-]_{S,P}$ transition matrix elements to the vacuum are proportional to the pion scalar and vector form factors. We assume that the $B^\pm \to \pi_2^+\pi_3^-$ matrix elements are expressed as products of the $B^\pm \to [\pi_2^+\pi_3^-]_{S,P}$ transition form factors by the relevant vertex function describing the decay of the $[\pi_2^+\pi_3^-]_{S,P}$ state into the final pion pair. The vertex functions are in turn assumed to be proportional to the pion scalar or vector form factors. In the present work, a single unitary function, namely the pion non-strange scalar form factor, describes then the three scalar resonances, $f_0(600)$, $f_0(980)$ and $f_0(1400)$ present in the $\pi^+\pi^-$ interaction.

In Sec. II we present the model used in the analysis. Sec. III is devoted to the construction of the pion scalar and vector form factors. The pertinent observables and the fitting procedure are described in Sec. IV while the results are discussed in Sec. V. A summary and some perspectives are outlined in the final Sec. VI.

II. DECAY AMPLITUDES

The amplitudes for the non-leptonic decays of the B meson are given as matrix elements of the effective weak Hamiltonian [6, 7]

$$H_{eff} = \frac{G_F}{\sqrt{2}} \sum_{p=u,c} \lambda_p \left[C_1 O_1^p + C_2 O_2^p + \sum_{i=3}^{10} C_i O_i + C_{7\gamma} O_{7\gamma} + C_{8g} O_{8g} \right] + h.c., \tag{1}$$

where

$$\lambda_u = V_{ub} V_{ud}^*, \ \lambda_c = V_{cb} V_{cd}^*, \tag{2}$$

the $V_{pp'}$ ($p' = b, d$) being Cabibbo-Kobayashi-Maskawa quark-mixing matrix elements. For the Fermi coupling constant G_F we take the value 1.16637×10^{-5} GeV^{-2}. The $C_i(\mu)$ are the Wilson coefficients of the four-quark operators $O_i(\mu)$ at a renormalization scale μ. The $O_{1,2}^p$ are left-handed current-current operators arising from W-boson exchange, $O_{i=3-10}$ are QCD and electroweak penguin operators involving a loop with a u or c quark and a W boson, $O_{7\gamma}$ and O_{8g} are the electromagnetic and chromomagnetic dipole operators [7].

Let p_B be the four-momentum of the $B^\pm$ meson and p_1 that of the isolated $\pi^\pm$. Let then p_2 denote the four-momentum of the π^+ and p_3 that of the π^- of the interacting $[\pi^+\pi^-]$ pair in the B rest frame. One has $p_B = p_1 + p_2 + p_3$ and we introduce the invariants $s_{ij} = (p_i + p_j)^2$ for $i, j = 1, 2, 3$ with $i < j$. For the $B^- \to \pi^- \, [\pi^+\pi^-]_{S,P}$ amplitude, we work in the center of mass frame of the $\pi^+\pi^-$ pair of pions with respective four-momenta p_2 and p_3 (or p_1 and p_2 for the symmetrized amplitudes). These two pions will be either in a relative S or P state. In the following we derive the amplitude for the $B^- \to \pi^- \, [\pi^+\pi^-]_{S,P}$ processes. The transcription to the $B^+ \to \pi^+ \, [\pi^+\pi^-]_{S,P}$ processes is straightforward. Applying the QCD factorization formula for the $B^- \to \pi^- \, [\pi^+\pi^-]_{S,P}$ process, the matrix elements of the effective weak Hamiltonian (1) can be written as [7]

$$\left\langle \pi^-(p_1) \, [\pi^+(p_2)\pi^-(p_3)]_{S,P} | H_{eff} | B^-(p_B) \right\rangle = \frac{G_F}{\sqrt{2}} \sum_{p=u,c} \lambda_p \left\langle \pi^- \, [\pi^+\pi^-]_{S,P} | T_p | B^- \right\rangle, \tag{3}$$

to which must be added the symmetrized term $\langle \pi^-(p_3)[\pi^+(p_2)\pi^-(p_1)]_{S,P} | H_{eff} | B^-(p_B) \rangle$. With $M_1 \equiv \pi^-$ and $M_2 \equiv [\pi^+\pi^-]_{S,P}$ or $M_1 \equiv [\pi^+\pi^-]_{S,P}$ while $M_2 \equiv \pi^-$, one has

$$
\begin{aligned}
\langle \pi^- \, [\pi^+\pi^-]_{S,P} | T_p | B^- \rangle \;=\; & \langle \pi^- \, [\pi^+\pi^-]_{S,P} | \Big\{ a_1(M_1M_2)\delta_{pu}(\bar{u}b)_{V-A} \otimes (\bar{d}u)_{V-A} \\
& + \; a_2(M_1M_2)\delta_{pu}(\bar{d}b)_{V-A} \otimes (\bar{u}u)_{V-A} + a_3(M_1M_2) \sum_q (\bar{d}b)_{V-A} \otimes (\bar{q}q)_{V-A} \\
& + \; a_4^p(M_1M_2) \sum_q (\bar{q}b)_{V-A} \otimes (\bar{d}q)_{V-A} + a_5(M_1M_2) \sum_q (\bar{d}b)_{V-A} \otimes (\bar{d}q)_{V+A} \\
& + \; a_6^p(M_1M_2) \sum_q (-2)(\bar{q}b)_{sc-ps} \otimes (\bar{d}q)_{sc+ps} \\
& + \; a_7(M_1M_2) \sum_q (\bar{d}b)_{V-A} \otimes \frac{3}{2} e_q (\bar{q}q)_{V+A} \\
& + \; a_8^p(M_1M_2) \sum_q (-2)(\bar{q}b)_{sc-ps} \otimes \frac{3}{2} e_q (\bar{d}q)_{sc+ps} \\
& + \; a_9(M_1M_2) \sum_q (\bar{d}b)_{V-A} \otimes \frac{3}{2} e_q (\bar{q}q)_{V-A} \\
& + \; a_{10}(M_1M_2) \sum_q (\bar{q}b)_{V-A} \otimes \frac{3}{2} e_q (\bar{d}q)_{V-A} \Big\} \, |B^-\rangle, \qquad (4)
\end{aligned}
$$

where a_j^p are effective QCDF coefficients. In Eq.(4), $(\bar{q}_1 q_2)_{V\mp A} = \bar{q}_1 \gamma_\mu (1 \mp \gamma_5) q_2$, $(\bar{q}_1 q_2)_{sc\pm ps} = \bar{q}_1 (1 \pm \gamma_5) q_2$ and e_q denotes the electric charge of the quark q in units of the elementary charge e. The sum on the index q runs over u and d and the summation over the color degree of freedom has been performed. The notations sc and ps stand for scalar and pseudoscalar, respectively.

At next-to-leading order (NLO) in the strong coupling constant α_s, the general expression of the a_i^p quantities in terms of effective Wilson coeffficients is [9]

$$
a_i^p(M_1M_2) = \left(C_i + \frac{C_{i\pm1}}{N_C} \right) N_i(M_2) + \frac{C_{i\pm1}}{N_C} \frac{C_F \alpha_s}{4\pi} \left[V_i(M_2) + \frac{4\pi^2}{N_C} H_i(M_1M_2) \right] + P_i^p(M_2), \qquad (5)
$$

where the upper (lower) signs apply when the index i is odd (even), N_C is the number of colors, $N_C = 3$ and $C_F = (N_C^2 - 1)/2N_C$. The sum over the color degree of freedom have been performed in Eq. (4). Note that in the leading-order (LO) contribution $N_i(M_2) = 0$ for $M_2 = [\pi^+\pi^-]_P$ and $i = 6, 8$, otherwise $N_i(M_2) = 1$. The NLO quantities $V_i(M_2)$ arise from one loop vertex corrections, $H_i(M_1M_2)$ from hard spectator scattering interactions and $P_i^p(M_2)$ from penguin contractions. Here the meson M_2 is the meson which does not include the spectator quark of the B meson. The superscript p in $a_i^p(M_1M_2)$ is to be omitted for $i = 1$, 2, 3, 5, 7 and 9 since the penguin corrections are equal to zero in these cases. In our calculation we shall not include the NLO hard scattering corrections which require the introduction of two phenomenological parameters to regularize end point divergences related to asymptotic wave functions [9].

In Eq. (4) the symbol $\otimes$ indicates that the different components of the matrix elements $\langle \pi^- \, [\pi^+\pi^-]_{S,P}|T_p|B^-\rangle$ are to be calculated in the factorized form,

$$\begin{aligned}\left\langle \pi^-(p_1)[\pi^+(p_2)\pi^-(p_3)]_{S,P} \; |j_1 \otimes j_2|B^-(p_B)\right\rangle \equiv \quad & \left\langle [\pi^+\pi^-]_{S,P}|j_1|B^-\right\rangle \left\langle \pi^- \; |j_2|0\right\rangle \text{ or} \\ & \left\langle \pi^-|j_1|B^-\right\rangle \left\langle [\pi^+\pi^-]_{S,P} \; |j_2|0\right\rangle , \end{aligned} \tag{6}$$

since we neglect B^- annihilation contributions which are expected to be small [6]. Furthermore, as for the hard scattering corrections, their evaluation [9] introduces two phenomenological parameters. In Eq. (6) j_1 and j_2 denote the appropriate quark currents entering in Eq. (4). Note that, in our approach, in the evaluation of the long distance matrix element $\langle [\pi^+\pi^-]_{S,P}|j_1|B^-\rangle$, we make the hypothesis that the transitions of B^- to the $[\pi^+\pi^-]_{S,P}$ states go first through intermediate meson resonances $R_{S,P}$ which then decay into a $\pi^+\pi^-$ pair. We describe these decays by a vertex function modeled by assuming them to be proportional to the pion scalar or vector form factors, respectively. For the short distance part of the decay amplitudes proportional to a combination of the effective coefficients $a_i^p(M_1M_2)$ it can be seen that for terms coming from the first line of the right hand side of Eq. (6) $M_1 \equiv [\pi^+\pi^-]_{S,P}$, $M_2 \equiv \pi^-$ and for those from the second line $M_1 \equiv \pi^-$ while $M_2 \equiv [\pi^+\pi^-]_{S,P}$. In the following, when $M_2 \equiv [\pi^+\pi^-]_{S,P}$, we assume that the NLO corrections $V_i(M_2)$ and $P_i^p(M_2)$ are evaluated at the meson resonances $R_{S,P}$ position. Here we take $R_P \equiv \rho(770)^0$ and $R_S \equiv f_0(980)$. A similar approximation has been applied in Refs. [3, 4] for the $[K\pi]_{S,P}$ states with $R_P \equiv K^*(892)$ and $R_S \equiv K_0^*(1430)$.

Introducing the short distance terms

$$\begin{aligned} u(R_{S,P}\pi^-) \; = \; & \lambda_u \left[a_1(R_{S,P}\pi^-) + a_4^u(R_{S,P}\pi^-) + a_{10}^u(R_{S,P}\pi^-) - \left(a_6^u(R_{S,P}\pi^-) + a_8^u(R_{S,P}\pi^-)\right) r_\chi^\pi\right] \\ & + \lambda_c \left[+a_4^u(R_{S,P}\pi^-) + a_{10}^c(R_{S,P}\pi^-) - \left(a_6^c(R_{S,P}\pi^-) + a_8^c(R_{S,P}\pi^-)\right) r_\chi^\pi\right], \end{aligned} \tag{7}$$

$$v(\pi^- R_S) = \lambda_u \left[-2a_6^u(\pi^- R_S) + a_8^u(\pi^- R_S)\right] + \lambda_c \left[-2a_6^c(\pi^- R_S) + a_8^c(\pi^- R_S)\right], \tag{8}$$

and

$$\begin{aligned} w(\pi^- R_P) \; = \; & \lambda_u \left[a_2(\pi^- R_P) - a_4^u(\pi^- R_P) + \frac{3}{2}\left(a_7(\pi^- R_P) + a_9(\pi^- R_P)\right) + \frac{1}{2}a_{10}^u(\pi^- R_P)\right] \\ & + \lambda_c \left[-a_4^c(\pi^- R_P) + \frac{3}{2}\left(a_7(\pi^- R_P) + a_9(\pi^- R_P)\right) + \frac{1}{2}a_{10}^c(\pi^- R_P)\right], \end{aligned} \tag{9}$$

one obtains, from Eqs. (3), (4) and (6), the following S- and P-wave matrix elements

$$\sum_{p=u,c} \lambda_p \left\langle \pi^-(p_1)[\pi^+(p_2)\pi^-(p_3)]_S|T_p|B^-\right\rangle = X_S\, u(R_S\pi^-) + Y_S\, v(\pi^- R_S), \tag{10}$$

$$\sum_{p=u,c} \lambda_p \left\langle \pi^-(p_1)[\pi^+(p_2)\pi^-(p_3)]_P|T_p|B^-\right\rangle = X_P\, u(R_P\pi^-) + Y_P\, w(\pi^- R_P). \tag{11}$$

In Eq. (7) the chiral factor r_χ^π is given by $r_\chi^\pi = 2m_\pi^2/[(m_b+m_u)(m_u+m_d)]$, m_u and m_d being the u and d quark masses, respectively. The long distance functions $X_{S,P}$ and $Y_{S,P}$, evaluated in appendix A, read

$$\begin{aligned}
X_S &\equiv \left\langle [\pi^+(p_2)\pi^-(p_3)]_S|(\bar u b)_{V-A}|B^-\right\rangle \left\langle \pi^-|(\bar d u)_{V-A}|0\right\rangle \\
&= -\sqrt{\frac{2}{3}}\,\chi_S\, f_\pi\, (M_B^2 - s_{23})\, F_0^{BR_S}(m_\pi^2)\, \Gamma_1^{n*}(s_{23}), &(12)\\
Y_S &\equiv \left\langle \pi^-|(\bar d b)_{sc-ps}|B^-\right\rangle \left\langle [\pi^+(p_2)\pi^-(p_3)]_S|(\bar d d)_{sc+ps}|0\right\rangle \\
&= \sqrt{\frac{2}{3}}\, B_0\, \frac{M_B^2 - m_\pi^2}{m_b - m_d}\, F_0^{B\pi}(s_{23})\, \Gamma_1^{n*}(s_{23}), &(13)\\
X_P &\equiv \left\langle [\pi^+(p_2)\pi^-(p_3)]_P|(\bar u b)_{V-A}|B^-\right\rangle \left\langle \pi^-|(\bar d u)_{V-A}|0\right\rangle \\
&= \frac{f_\pi}{f_{R_P}}\, (s_{13} - s_{12})\, A_0^{BR_P}(m_\pi^2)\, F_1^{\pi\pi}(s_{23}), &(14)\\
Y_P &\equiv \left\langle \pi^-|(\bar d b)_{V-A}|B^-\right\rangle \left\langle [\pi^+(p_2)\pi^-(p_3)]_P|(\bar u u)_{V-A}|0\right\rangle \\
&= (s_{13} - s_{12}) F_1^{B\pi}(s_{23}) F_1^{\pi\pi}(s_{23}), &(15)
\end{aligned}$$

where χ_S represents the S-wave strength parameter which will be fitted. To reduce the number of parameters, we do not introduce here the possible R_S dependence of χ_S and of $F_0^{BR_S}(m_\pi^2)$. We expect this R_S dependence to be stronger in the pion scalar form factor $\Gamma_1^{n*}(s)$. For the pion decay constant we take $f_\pi = 0.1304$ GeV [18]. The R_P decay constant is denoted by f_{R_P} and the B-meson mass by M_B. Since the $\pi^+\pi^-$ P-wave is largely dominated by the $\rho(770)$ meson we choose $f_{R_P} = f_\rho = 0.209$ GeV [9]. The quantity $B_0 = -2\,\langle 0|\bar q q|0\rangle/f_\pi^2$ is proportional to the quark condensate. We calculate it as $B_0 \simeq m_\pi^2/(m_u+m_d)$. At the renormalization scale $\mu = m_b/2$ we use $m_b = 4.9$ GeV and $m_u = m_d = 0.005$ GeV. For the transition form factor between the B meson and R_S state we take $F_0^{BR_S}(m_\pi^2) = 0.13$ [19] and for that between the B meson and R_P state $A_0^{BR_P}(m_\pi^2) = 0.37$ [20]. For the $B\pi$ scalar and vector transition form factors $F_0^{B\pi}(s)$ and $F_1^{B\pi}(s)$, we use the following light-cone sum rule parametrization developed in appendix A of Ref. [21], viz.

$$F_0^{B\pi}(s) = \frac{0.258}{1 - s/s_0}, \tag{16}$$

$$F_1^{B\pi}(s) = \frac{0.744}{1 - s/M_{B^*}^2} - \frac{0.486}{1 - s/s_1}, \tag{17}$$

with $s_0 = 33.81$ GeV^2, $M_{B^*} = 5.32$ GeV and $s_1 = 40.73$ GeV^2. The pion non-strange scalar and vector form factors $\Gamma_1^{n*}(s)$ and $F_1^{\pi\pi}(s)$ will be discussed in the next section. Note that [27]

$$\Gamma_1^{n*}(s) = \frac{\sqrt{3}}{2B_0} \left\langle [\pi^+\pi^-]_S | \bar{n}n | 0 \right\rangle, \tag{18}$$

with $\bar{n}n = \frac{1}{\sqrt{2}}(\bar{u}u + \bar{d}d)$.

In summary, from the S- and P-wave matrix elements (10) and (11), we obtain the total symmetrized amplitude for the $B^- \to \pi^+\pi^-\pi^-$ decay as

$$\mathcal{M}_{sym}^-(s_{12}, s_{23}) = \frac{1}{\sqrt{2}} \left[\mathcal{M}_S^-(s_{12}) + \mathcal{M}_S^-(s_{23}) + \mathcal{M}_P^-(s_{12})(s_{13} - s_{23}) + \mathcal{M}_P^-(s_{23})(s_{13} - s_{12}) \right], \tag{19}$$

with

$$\mathcal{M}_S^-(s_{ij}) = \frac{G_F}{\sqrt{3}} \left[-\chi_S f_\pi \left(M_B^2 - s_{ij} \right) F_0^{BR_S}(m_\pi^2) u(R_S\pi^-) + B_0 \frac{M_B^2 - m_\pi^2}{m_b - m_d} F_0^{B\pi}(s_{ij}) v(\pi^- R_S) \right] \Gamma_1^{n*}(s_{ij}) \tag{20}$$

and

$$\mathcal{M}_P^-(s_{ij}) = \frac{G_F}{\sqrt{2}} \left[\frac{f_\pi}{f_{R_P}} A_0^{BR_P}(m_\pi^2) u(R_P\pi^-) + F_1^{B\pi}(s_{ij}) w(\pi^- R_P) \right] F_1^{\pi\pi}(s_{ij}). \tag{21}$$

For the fully symmetrized $B^+ \to \pi^+\pi^-\pi^+$ decay amplitude we have

$$\mathcal{M}_{sym}^+(s_{12}, s_{23}) = \frac{1}{\sqrt{2}} \left[\mathcal{M}_S^+(s_{12}) + \mathcal{M}_S^+(s_{23}) + \mathcal{M}_P^+(s_{13})(s_{13} - s_{23}) + \mathcal{M}_P^+(s_{23})(s_{13} - s_{12}) \right], \tag{22}$$

with

$$\mathcal{M}_{S,P}^+(s_{ij}) = \mathcal{M}_{S,P}^- \left(s_{ij}, \lambda_u \to \lambda_u^*, \lambda_c \to \lambda_c^*, B^- \to B^+ \right). \tag{23}$$

III. SCALAR AND VECTOR FORM FACTORS

As shown in Ref. [22] the full knowledge of strong interaction meson-meson form factors is available if the meson-meson interaction is known at all energies. The calculation of the S- and

P-wave amplitudes (20) and (21) requires the values of the scalar and vector $B\pi$, $B(\pi\pi)$ and pion form factors. The knowledge of the $B \to \pi$ and $B \to [\pi\pi]_{S,P}$ transition form factors is needed far below the $B\pi$ and $B[\pi\pi]_{S,P}$ scattering region. One has then to rely on theoretical models constrained by experiment, as we do here for the $B[\pi\pi]_S$ form factor, using the value (see above in the previous section) determined in Ref. [19]. One could also use covariant light-front model, like that of Ref. [23] or, if avalaible, semi-leptonic decay analysis results. For the $B\pi$ form factors we take the QCD light-cone sum rule results of Ref. [21] recalled above in Eqs. (16) and (17). The special case of the pion form factors is developed below.

A. The pion scalar form factor

In the $\pi\pi$ case, the low-energy S wave being known and modeling the high-energy part one can rely on the Muskhelishvili-Omnès equations [24] to build up the pion scalar form factors. Their evaluation from these equations has been discussed in Ref. [25] and followed and developed in Ref. [26]. However here, we shall use another approach, initiated in Ref. [27] and applied, using a different $\pi\pi$ scattering matrix, in Ref. [1]. Extending this last work by introducing three channels and keeping the off-shell contributions, the pion scalar form factor $\Gamma_1^{n*}(s)$ entering in the S-wave amplitude Eq. (20) is modeled according to the following relativistic three coupled-channel equations

$$\Gamma_i^{n*}(s) = R_i^n(E) + \sum_{j=1}^{3} R_j^n(E) H_{ij}(E), \quad i = 1, 2, 3, \tag{24}$$

with

$$H_{ij}(E) = \int \frac{d^3p}{(2\pi)^3} T_{ij}(E, k_i, p) \frac{1}{E - 2\sqrt{p^2 + m_j^2} + i\epsilon} \frac{k_i^2 + \kappa^2}{p^2 + \kappa^2}, \tag{25}$$

where E represents the total energy, i.e., in the $\pi\pi$ center of mass, $E = \sqrt{s}$ and p is the off-shell momentum. In Eqs (24) and (25), the indices $i, j = 1, 2, 3$ refer to the $\pi\pi$, $K\bar{K}$ and effective $(2\pi)(2\pi)$ channels, respectively. The center of mass momenta are $k_j = \sqrt{s/4 - m_j^2}$, with $m_1 = m_\pi$, $m_2 = m_K$ and $m_3 = m_{(2\pi)}$. The T matrix is the corresponding three-channel two-body scattering matrix. Here we use the solution A of the three-coupled channel model of Refs. [28, 29], where the effective $m_{(2\pi)}$= 700 MeV. The functions $R_i^n(E)$ are the production functions responsible for the formation of the meson pairs before their scattering. From Eqs. (24) and (25) one can check that

$$Im\ \Gamma_i^{n*}(s) = -\sum_{j=1}^{3} \frac{k_j\sqrt{s}}{8\pi} T_{ji}^*(E,k_j,k_i)\Gamma_j^{n*}(s)\theta(\sqrt{s}-2m_j). \tag{26}$$

This is the same unitary relation as that of the corresponding Muskhelishvili-Omnès pion scalar form factors constructed in Ref. [26] [see Eq. (28) therein].

In Eq. (25) the regulator function $(k_i^2+\kappa^2)/(p^2+\kappa^2)$, which reduces to 1 on-shell ($k_i = p$), ensures the convergence of the integral. The range parameter κ will be fitted to data. The choice of a separable form for the interaction yields analytic expressions for the T matrix elements. One introduces a rank-2 separable potential in the $\pi\pi$ channel and a rank-1 separable potential in the $K\bar{K}$ and in the $(2\pi)(2\pi)$ ones. According to the formalism developed in Ref. [30] and applied in Ref. [28] one has for the T matrix elements:

$$\begin{aligned}
T_{11}(E,p,k_1) &= g_0(k_1)t_{00}(E)g_0(p) + g_1(k_1)t_{11}(E)g_1(p) + g_0(k_1)t_{10}(E)g_1(p) + g_1(k_1)t_{01}(E)g_0(p),\\
T_{21}(E,p,k_1) &= g_0(k_1)t_{02}(E)g_2(p) + g_1(k_1)t_{12}(E)g_2(p),\\
T_{31}(E,p,k_1) &= g_0(k_1)t_{03}(E)g_3(p) + g_1(k_1)t_{13}(E)g_3(p),
\end{aligned} \tag{27}$$

where

$$\begin{aligned}
g_0(k_1) &= \sqrt{\frac{4\pi}{m_\pi}}\frac{1}{k_1^2+\beta_0^2},\\
g_j(k_i) &= \sqrt{\frac{4\pi}{m_i}}\frac{1}{k_i^2+\beta_j^2}, \quad j=1,2,3.
\end{aligned} \tag{28}$$

The parameters β_j, $j = 0,1,2,3$, of the separable form of the scattering T matrix are given in Table 1 of Ref. [28] (fit A).

One can extend the expressions of the reduced symmetric $t(E)$ matrix elements given in terms of the separable potential parameters in appendix A of Ref. [30] to the case of Ref. [28] which we use here. The Yamaguchi form [31] of the $g_0(p)$ and $g_i(p)$ (28) in the T matrix elements (27) leads the following analytic expression for $\Gamma_i^{n*}(s)$ in Eq. (24)

$$\begin{aligned}
\Gamma_1^{n*}(s) =& R_1^n(E) + R_1^n(E)\{[t_{00}(E)g_0(k_1) + t_{01}(E)g_1(k_1)]g_0(k_1)F_{10}(k_1)+\\
&[t_{11}(E)g_1(k_1) + t_{10}(E)g_0(k_1)]g_1(k_1)F_{11}(k_1)\}+\\
&R_2^n(E)[g_0(k_1)t_{02}(E) + g_1(k_1)t_{12}(E)]g_2(k_2)F_{22}(k_2)+\\
&R_3^n(E)[g_0(k_1)t_{03}(E) + g_1(k_1)t_{13}(E)]g_3(k_3)F_{33}(k_3),
\end{aligned} \tag{29}$$

where

$$
\begin{aligned}
F_{10}(k_1) &= \frac{I_{1,0}(k_1)}{g_0(k_1)h_0(k_1)}, \\
F_{11}(k_1) &= \frac{I_{1,1}(k_1)}{g_1(k_1)h_1(k_1)}, \\
F_{22}(k_2) &= \frac{I_{2,2}(k_2)}{g_2(k_2)h_2(k_2)}, \\
F_{33}(k_3) &= \frac{I_{3,3}(k_3)}{g_3(k_3)h_3(k_3)},
\end{aligned}
\tag{30}
$$

with

$$
\begin{aligned}
h_i(k_i) &= \sqrt{\frac{4\pi}{m_i}}\frac{1}{k_i^2+\kappa^2}, \quad i=1,2,3, \\
h_0(k_1) &= h_1(k_1),
\end{aligned}
\tag{31}
$$

and

$$
I_{i,j}(k_i) = \int \frac{d^3p}{(2\pi)^3}\, g_j(p)\, \frac{1}{E-2\sqrt{p^2+m_i^2}+i\epsilon} h_i(p),
\tag{32}
$$

where $E=2\sqrt{k_i^2+m_i^2}$, $i=1,2,3$. The analytical expression for these integrals can be found in Appendix A of Ref. [30].

As in Ref. [27] one constraints the $\Gamma_i^{n*}(s)$ to satisfy the low energy behavior given by next-to-leading order one loop calculation in chiral perturbation theory (ChPT). One writes the expansion at low s as

$$
\Gamma_i^n(s) \cong d_i^n + f_i^n s, \quad i=1,2,3,
\tag{33}
$$

with real coefficients, $\Gamma_i^n(s)$ being real below the $\pi\pi$ threshold. Using the expressions obtained in NLO in ChPT for the $\Gamma_i^{n*}(s)$ given in Refs. [27, 32] one gets,

$$
\begin{aligned}
d_1^n &= \sqrt{\frac{3}{2}}\left[1+\frac{16m_\pi^2}{f^2}(2L_8^r-L_5^r)+8\frac{2m_K^2+3m_\pi^2}{f^2}(2L_6^r-L_4^r)\right. \\
&\quad \left. +\frac{m_\pi^2}{36\pi^2f^2}+\frac{m_\pi^2}{16\pi^2f^2}\log\frac{m_\pi^2}{\nu^2}-\frac{1}{96\pi^2f^2}\left(\frac{m_\pi^2}{3}+m_\eta^2\right)\log\frac{m_\eta^2}{\nu^2}\right], \\
f_1^n &= \sqrt{\frac{3}{2}}\left[\frac{4}{f^2}(2L_4^r+L_5^r)-\frac{1}{16\pi^2f^2}\left(1+\log\frac{m_\pi^2}{\nu^2}\right)\right. \\
&\quad \left. -\frac{1}{64\pi^2f^2}\left(1+\log\frac{m_K^2}{\nu^2}\right)-\frac{m_\pi^2}{192\pi^2f^2}\left(\frac{1}{m_\pi^2}-\frac{1}{9m_\eta^2}\right)\right],
\end{aligned}
\tag{34}
$$

and

$$
\begin{aligned}
d_2^n &= \frac{1}{\sqrt{2}}\left[1+\frac{m_\eta^2}{48\pi^2 f^2}\log\frac{m_\eta^2}{\nu^2}+\frac{16m_K^2}{f^2}\left(2L_8^r-L_5^r\right)+8\frac{6m_K^2+m_\pi^2}{f^2}\left(2L_6^r-L_4^r\right)\right.\\
&\left.+\frac{m_K^2}{72\pi^2 f^2}\left(1+\log\frac{m_\eta^2}{\nu^2}\right)\right],\\
f_2^n &= \frac{1}{\sqrt{2}}\left[\frac{4}{f^2}\left(2L_4^r+L_5^r\right)-\frac{1}{64\pi^2 f^2}\left(1+\log\frac{m_\eta^2}{\nu^2}\right)-\frac{m_K^2}{432\pi^2 f^2}\frac{1}{m_\eta^2}\right.\\
&\left.-\frac{3}{64\pi^2 f^2}\left(1+\log\frac{m_K^2}{\nu^2}\right)-\frac{3}{64\pi^2 f^2}\left(1+\log\frac{m_\pi^2}{\nu^2}\right)\right],
\end{aligned}
\tag{35}
$$

ν being the scale of dimensional regularization and $f=f_\pi/\sqrt{2}$. Furthermore for the ChPT low-energy constants, L_k^r, $k=4,5,6,8$, we use the recent determinations of lattice QCD at $\nu=1$ GeV as given in Table X of Ref. [33]. For $f=92.4$ MeV, we obtain $d_1^n=1.1957$, $f_1^n=3.1329$ GeV^{-2}, $d_2^n=0.7193$ and $f_2^n=1.6719$ GeV^{-2}. Here we assume $\Gamma_3^n(0)=0$ which leads to $d_3^n=0$ and we also assume $f_3^n=0$.

The real production functions are parametrized as

$$
R_i^n(E)=\frac{\alpha_i^n+\tau_i^n E+\omega_i^n E^2}{1+cE^4},\ i=1,2,3, \tag{36}
$$

the fitted parameter c controling the high energy behavior. The other parameters, α_i^n, τ_i^n and ω_i^n are calculated by requiring that $\Gamma_i^n(s)$ in Eq. (24) has the low energy expansion Eq. (33). These nine parameters satisfy a linear system of nine equations displayed in appendix B. Their numerical values, depending on the value of the range parameter κ [see Eq. (28)], will be given in Sec. V.

B. The pion vector form factor

As for the scalar case one could use the Muskhelishvili-Omnès equations to built up the pion vector form factor. This was done in Ref. [3] for the $K\pi$ vector form factor. Here, noting that the knowledge of this form factor is required to describe the $\tau^-\to\pi^-\pi^0\nu_\tau$ decay, we shall use the phenomenological model of the Belle Collaboration [34]. Fitting their high statistics data, they built the pion vector form factor $F_1^{\pi\pi}(s_{23})$ by including the contribution of the three vector resonances $\rho(700)$, $\rho(1450)$ and $\rho(1700)$. Here we use the parameters given in the third column of Table VII of Ref. [34].

IV. OBSERVABLES AND DATA FITTING

A. Physical observables

The symmetrized $B^- \to \pi_1^-\pi_2^+\pi_3^-$ amplitude (19) depends on the two effective $\pi\pi$ masses, $m_{12} = \sqrt{s_{12}}$ and $m_{23} = \sqrt{s_{23}}$ of the Dalitz plot. In the center of mass of $\pi^-(p_1)$ and $\pi^+(p_2)$, the pion momenta fulfill the equations

$$\begin{aligned} |\overrightarrow{p_1}| &= \frac{1}{2}\sqrt{m_{12}^2 - 4m_\pi^2}, \qquad\qquad |\overrightarrow{p_2}| = |\overrightarrow{p_1}|, \\ |\overrightarrow{p_3}| &= \frac{1}{2m_{12}}\sqrt{\left[M_B^2 - (m_{12}+m_\pi)^2\right]\left[M_B^2 - (m_{12}-m_\pi)^2\right]}, \end{aligned} \tag{37}$$

and the cosine of the helicity angle θ between the direction of $\overrightarrow{p_2}$ and that of $\overrightarrow{p_3}$ reads

$$\cos\theta = \frac{1}{2|\overrightarrow{p_2}||\overrightarrow{p_3}|}\left[-m_{23}^2 + \frac{1}{2}\left(M_B^2 - m_{12}^2 + 3m_\pi^2\right)\right]. \tag{38}$$

For fixed values of the effective mass m_{12}, the variables $\cos\theta$ and m_{23} are equivalent.

The double differential $B^- \to \pi^-\pi^+\pi^-$ branching fraction is

$$\frac{d^2\mathcal{B}^-}{dm_{12}\; d\cos\theta} = \frac{1}{\Gamma_B}\frac{m_{12}|\overrightarrow{p_2}||\overrightarrow{p_3}|}{8(2\pi)^3 M_B^2}\left|\mathcal{M}_{sym}^-(s_{12}, s_{23})\right|^2, \tag{39}$$

where Γ_B is the total width of the B^-. Since the Dalitz plot is symmetric under the interchange of m_{12} and m_{23}, one can limit the integration range on m_{23} to the values larger than m_{12}; hence, the differential effective mass distribution reads

$$\frac{d\mathcal{B}^-}{dm_{12}} = \int_{-1}^{\cos\theta_g} \frac{d^2\mathcal{B}^-}{dm_{12}\; d\cos\theta} d\cos\theta, \tag{40}$$

where $\cos\theta_g$ corresponds to the value of $\cos\theta$ in Eq. (38) with $m_{12} = m_{23}$, viz.,

$$\cos\theta_g = \frac{1}{4|\overrightarrow{p_2}||\overrightarrow{p_3}|}\left(M_B^2 - 3m_{12}^2 + 3m_\pi^2\right). \tag{41}$$

The variable m_{12} in Eq. (40) is also called the light (or minimal) effective mass m_{min} while m_{23} is the heavy (or maximal) effective mass, m_{max}. The $B^- \to \pi^-\pi^+\pi^-$ branching fraction is then twice the integral of the differential branching fraction (40) over m_{12}.

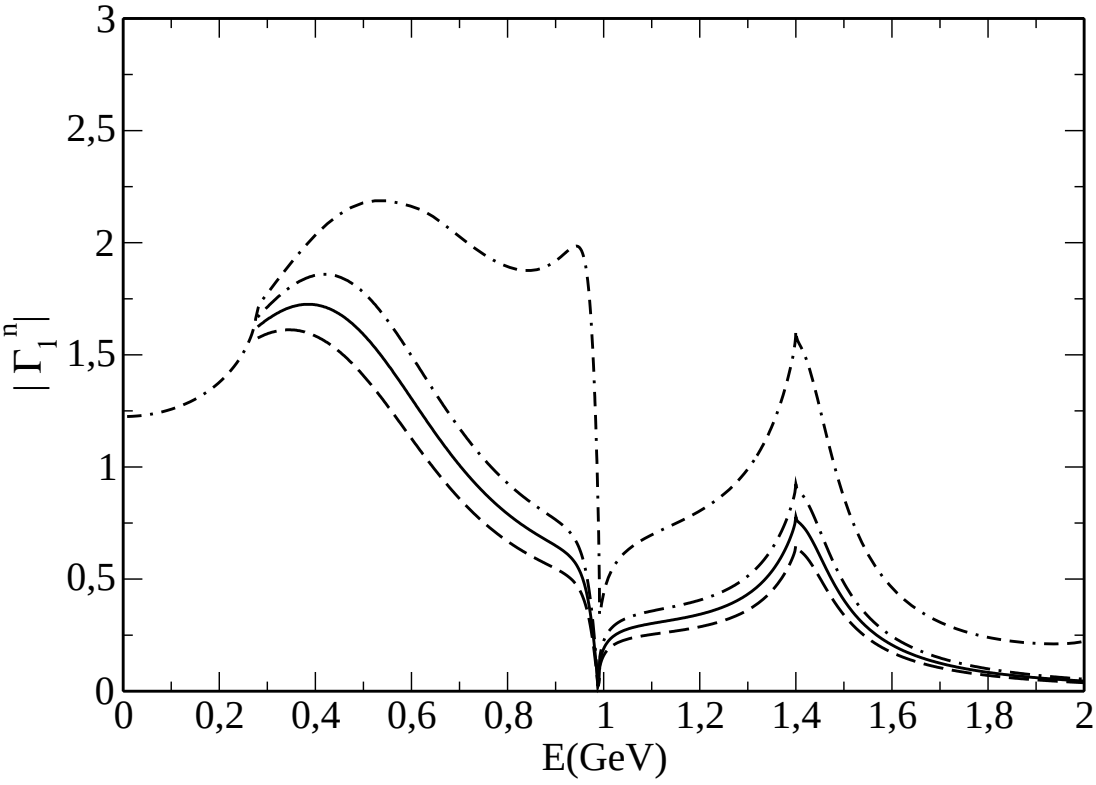

FIG. 1: Modulus of the pion scalar form factor Γ_1^n (solid line), obtained in our fit using the NLO a_i^p with $\kappa = 5$ GeV and for which the fitted parameter $c = 31.5$ GeV^{-4}, compared to that calculated in Ref. [26] using the Muskhelishvili-Omnès equations (doubled-dashed dot line). The dashed-dot line (for $c = 26.5$ GeV^{-4}) and the dashed one (for $c = 37.7$ GeV^{-4}) represent the variation of the Γ_1^n modulus when c varies within its error band.

B. Data fitting

We aim at describing the experimental $\pi^+\pi^-$ distributions obtained by the BABAR Collaboration in the Dalitz plot analysis of the $B^\pm \to \pi^\pm\pi^\pm\pi^\mp$ decays [5]. Two different background distributions, related to the $q\bar{q}$ and the $B\bar{B}$ components, are subtracted from Fig. 4 of Ref. [5]. Six light effective $\pi^+\pi^-$ mass distributions are extracted for B^+ and B^- decays with a subdivision of the data into positive and negative values of the cosine of the helicity angle θ. For the B^+ and B^- distributions we reject two data points corresponding to the $\pi^+\pi^-$ effective masses equal to 485 and 515 MeV. Also two points at 470 and 530 MeV for the four mass distributions with $\cos\theta > 0$ or with $\cos\theta < 0$ are not taken into account. This is done to exclude the possible contribution of

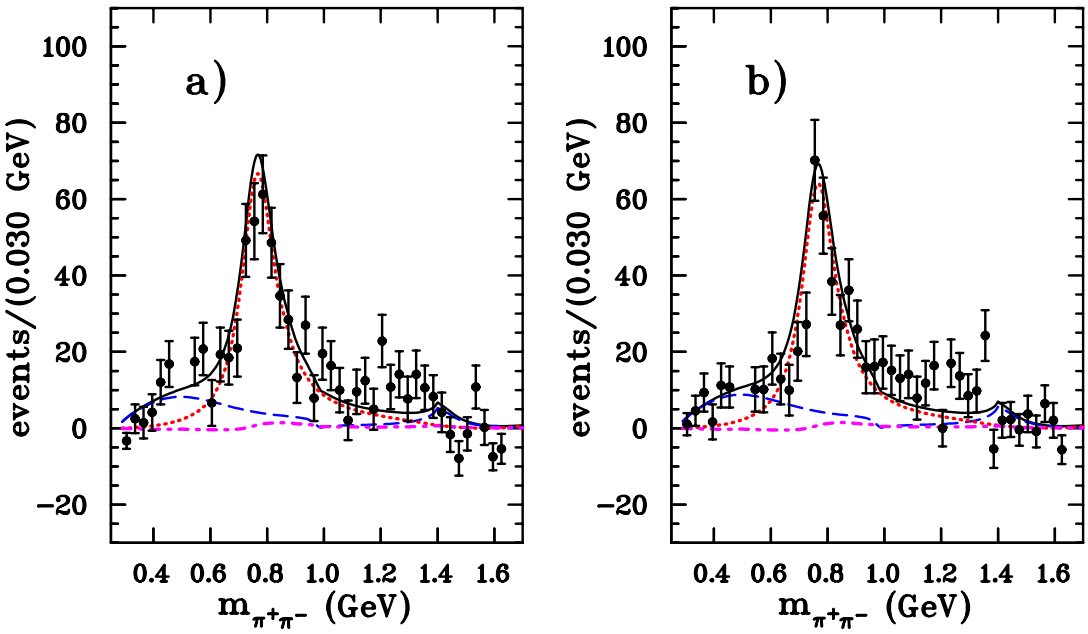

FIG. 2: The $\pi^+\pi^-$ light effective mass distributions from the fit to the BABAR experimental data [5], a) for the B^- decays and b) for the B^+ decays. The dashed line represents the S-wave contribution of our model, the dotted line that of the P wave and the dot-dashed line that of the interference term. The solid line corresponds to the sum of these contributions.

the decay processes $B^\pm \to K^0_S\pi^\pm$.

As a by-product of the background subtraction, five data points, with a small number of events, have negative values with small statistical errors. For these five data points we increase their errors to values corresponding to those of the points lying in a close vicinity. This is done at 1385 MeV for the B^- distribution, at 1475 MeV for the B^+ one, at 290 and 1610 MeV for the B^- distribution with $\cos\theta > 0$ and at 1490 MeV for the B^- one with $\cos\theta < 0$.

We perform a χ^2 fit to the 170 data points corresponding to the six invariant mass distributions described above. The theoretical distributions are normalized to the number of experimental events in the analyzed range from 290 up to 1640 MeV. In the fits, done for a fixed value of the range parameter κ entering Eqs. (28), the following parameters were varied: the production functions $R^n_i(E)$ [Eq. (36)] parameter c, the real S-wave strength parameter χ_S and the real P-wave normalization parameter N_P. For both B^- and B^+ decays, the first two parameters enter in the S-wave part of the decay amplitude and the third one multiplies the P-wave amplitudes [see Eqs. (20), (21) and (23)].

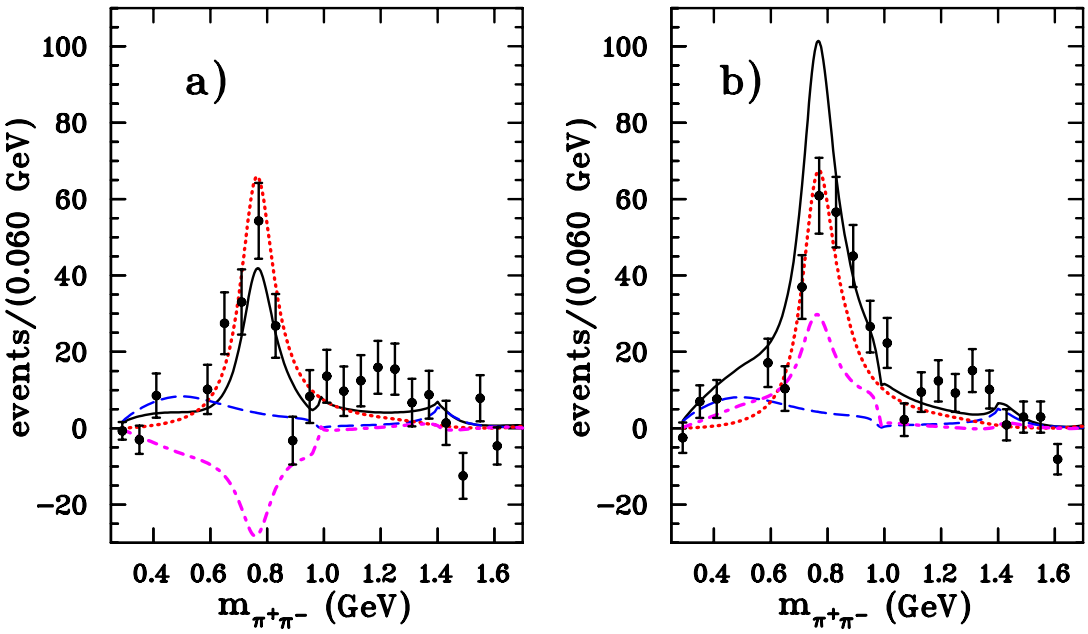

FIG. 3: As in Fig. 2 but for the B^- decays a) with $\cos\theta < 0$ and b) with $\cos\theta > 0$.

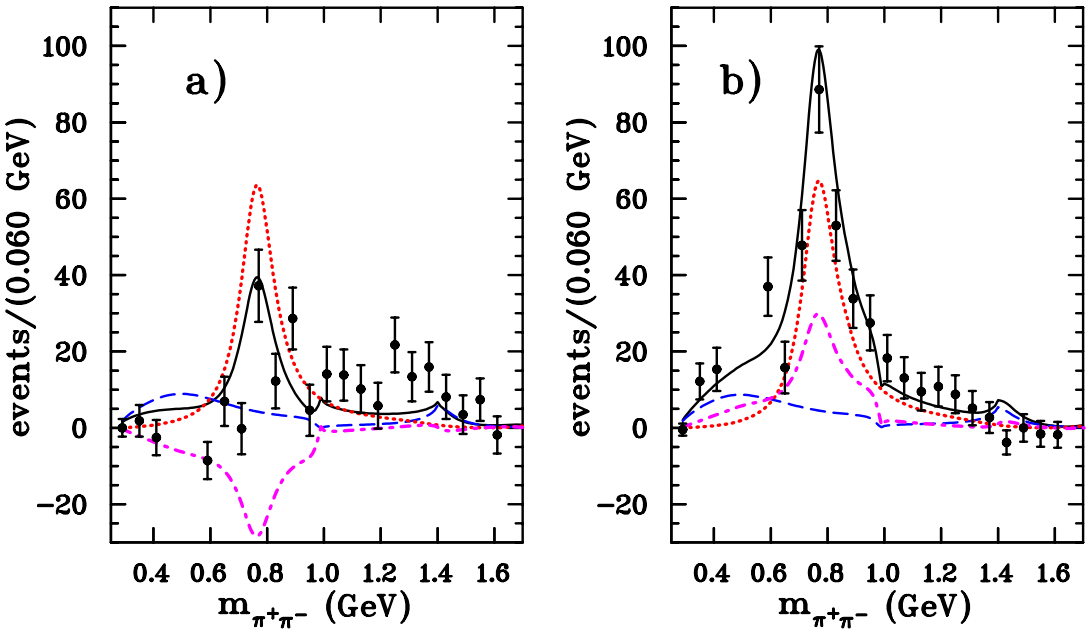

FIG. 4: As in Fig. 3 but for the B^+ decays.

V. RESULTS AND DISCUSSION

In the fits to the selected BABAR data as described in the previous section, the CKM matrix elements [see Eq. (2)] are calculated with $\lambda = 0.2257$, $A = 0.814$, $\bar{\rho} = 0.135$ and $\bar{\eta} = 0.349$ [18] which leads to $\lambda_u = 1.26 \times 10^{-3} - i\ 3.27 \times 10^{-3}$ and $\lambda_c = -9.35 \times 10^{-3} - i\ 1.72 \times 10^{-6}$. The LO

TABLE I: Leading order (LO) and next-to-leading order (NLO) coefficients $a_i^p(R_{S,P},\pi^-)$, $a_i^p(\pi^-,R_S)$ and $a_i^p(\pi^-,R_P)$ [see Eq. (5)] entering into $u(R_{S,P}\pi^-)$ [Eq. (7)], $v(\pi^-R_S)$[Eq. (8)] and $w(\pi^-R_P)$ [Eq. (9)], respectively. The NLO coefficients are the sum of the LO coefficients plus next-to-leading order vertex and penguin corrections. Here the renormalization scale is $\mu = m_b/2$. The superscript p is omitted for $i = 1$, 2, 3, 5, 7 and 9, the penguin corrections being zero for these cases.

	$a_i^p(R_{S,P}\pi^-)$		$a_i^p(\pi^-R_S)$		$a_i^p(\pi^-R_P)$	
	LO	NLO	LO	NLO	LO	NLO
a_1	1.039	$1.071 + i0.03$				
a_2					0.084	$-0.041 - i0.114$
a_4^u	-0.044	$-0.032 - i0.019$			-0.044	$-0.032 - i0.019$
a_4^c	-0.044	$-0.039 - i0.007$			-0.044	$-0.039 - i0.007$
a_6^u	-0.062	$-0.057 - i0.017$	-0.062	$-0.075 - i0.017$		
a_6^c	-0.062	$-0.062 - i0.004$	-0.062	$-0.079 - i0.004$		
a_7					0.0001	$0.0 + i0.0001$
a_8^u	0.0007	$0.0008 + i0.0$	0.0007	$0.0007 + i0.0$		
a_8^c	0.0007	$0.0008 + i0.0$	0.0007	$0.0007 + i0.0$		
a_9					-0.0094	$-0.0097 - i0.0003$
a_{10}^u	-0.0009	$0.0006 + i0.0010$			-0.0009	$0.0006 + i0.0010$
a_{10}^c	-0.0009	$0.0006 + i0.0010$			-0.0009	$0.0006 + i0.0010$

contributions of the Wilson coefficients to the a_i^p Eq. (5) are given in the second, fourth and sixth columns of Table I. The sum of the leading order coefficient plus the next-to-leading order vertex and penguin corrections for the a_i^p coefficients, entering into $u(R_{S,P}\pi^-)$ [Eq. (7)], $v(\pi^-R_S)$[Eq. (8)] and $w(\pi^-R_P)$ [Eq. (9)], are displayed in columns three, five and seven, respectively. The corrections are calculated according to Refs. [7] and [9] using the Gegenbauer moments for pions taken from the Table 2 of Ref. [7] and the corresponding moments for the ρ meson from Table 1 of Ref. [35]. In the calculation of the coefficients $a_6^p(\pi^-R_S)$ and $a_8^p(\pi^-R_S)$, contributing to $v(\pi^-R_S)$, we apply the method explained in appendix A of Ref. [11]. Here the renormalization scale $\mu = m_b/2$ and we take for the strong coupling constant $\alpha_s(m_b/2) = 0.303$.

There are four free parameters at our disposal. Two of them, the regulator range κ and the high energy cut-off c of the production functions [Eq. (36)] are linked to the determination of the S-wave Γ_1^n form factor. The other two, χ_S and N_P are related to the strength of the S and P amplitudes, respectively. The range κ should be larger than the upper limit ~ 1.7 GeV of the effective $m_{\pi\pi}$ used here. In our fits we find that the total χ^2 decreases when κ increases and that

TABLE II: Parameters of the production function $R_i^n(E)$ Eq. (36) for $\kappa = 5$ GeV

i	α_i^n	τ_i^n (GeV^{-1})	ω_i^n (GeV^{-2})
1	0.5361	-0.2101	1.2478
2	0.5455	0.0753	1.4115
3	1.1308	0.3765	3.0436

for κ beyond 5 GeV the improvement is smaller than 1. So we fix the range parameter κ to be 5 GeV. We perform thus two fits for the full $S+P$-wave amplitude calculated with the NLO and with the LO a_i^p coefficients. Hereafter the quoted results given inside parentheses correspond to the numbers obtained in the second fit.

A good overall agreement with BABAR 's data is achieved with $c = 31.5^{+6.2}_{-5.0}$ $\left(30.4^{+6.1}_{-5.2}\right)$ GeV^{-4}, $\chi_S = -18.3^{+2.5}_{-2.3}$ (-18.4 ± 2.5) GeV^{-1} and $N_P = 1.132^{+0.034}_{-0.035}$ (1.017 ± 0.031). The total χ^2 is equal to 321.3 (321.5) for the 170 experimental points of the fit. For both fits the branching fraction for the $B^\pm \to \rho(770)^0\pi^\pm$, $\rho(770)^0 \to \pi^+\pi^-$ decay is $(8.2 \pm 0.5\times)10^{-6}$, to be compared with the BABAR Collaboration determination of $(8.1 \pm 0.7 \pm 1.2^{+0.4}_{-1.1}) \times 10^{-6} \approx (8.1 \pm 1.6) \times 10^{-6}$ from their isobar model analysis [5]. Note that for the LO fit we explain essentially the BABAR Collaboration's result without significant modification of the normalization, the parameter $N_P \approx 1.02$ being close to 1. For the NLO fit, $N_P \approx 1.13 \pm 0.03$ and one can compare $N_P^2 - 1 \approx 28\%$ with the average 20% error of the experimental branching ratio.

The CP average total branching fraction of the $B^\pm \to \pi^\pm\pi^\mp\pi^\pm$ decays calculated in the NLO fit is equal to $(13.2 \pm 1.4) \times 10^{-6}$ to be compared to the measured value of $\left(15.2 \pm 0.6 \pm 1.2^{+0.4}_{-0.3}\right) \times 10^{-6}$ (table III of Ref. [5]). The S-wave contribution represents here as much as 25% of the total branching fraction. This contribution is larger than that of the $\rho(1450)$ and $\rho(1700)$ which represents only 15 % of the total P-wave contribution.

Before comparing our effective mass distributions to the experimental ones, we now give our result for the pion scalar form factor $\Gamma_1^n(s)$. With the fixed value of $\kappa = 5$ GeV used in the fits, one obtains for the α_i^n, τ_i^n and ω_i^n, $i = 1, 2, 3$, entering into Eq. (36), the values given in Table II. Then, in Fig. 1, the modulus of the corresponding $\Gamma_1^n(s)$ obtained using the NLO coefficients a_i^p and for which the fitted parameter $c = 31.5$ GeV^{-4} is compared to that calculated by Moussallam [36] solving the Muskhelishvili-Omnès equations [26] with a high-energy ansatz starting at 2 GeV and the same low-energy three coupled-channel scattering T matrix as in our model (see Sec. III A). However, in his calculation the off-diagonal matrix elements $T_{13}(E, k_i, p)$ and $T_{23}(k_i, E, p)$ are set

to zero in the unphysical region $E < 2m_3 = 1.4$ GeV. Let us remind here that the imaginary parts of these two pion form factors satisfy exactly the same relation given by Eq. (26). The functional dependence of both $\Gamma_1^{n*}(s)$ moduli is quite similar. It can be seen in Fig. 1 that, within our model, the needed $\Gamma_1^{n*}(s)$ is relatively well constrained. Let us note that if we choose $\kappa = 3$ GeV then the moduls of $\Gamma_1^{n*}(s)$ is slightly larger than that for $\kappa = 5$ GeV. Then one obtains $c = 19.7$ GeV^{-4}, $\chi_S = -17.6$ GeV^{-1} with a total χ^2 of 326.

For $E = \sqrt{s}$ close to zero the behavior of our pion form factor is governed by the chiral perturbation expansion Eq. (33). These ChPT constraints, not explicitly included in Moussallam's case, lead to $\Gamma_1^{n*}(s)$ moduli of both approaches to differ only slightly near the $\pi\pi$ threshold. Above the $\pi\pi$ threshold, there is a maximum corresponding to the $f_0(600)$ resonance, then follows, close to 1 GeV, a characteristic dip due to the $f_0(980)$ and finally, below the spike at 1.4 GeV related to the opening of the third channel, there is some enhancement generated by the $f_0(1400)$ present in the $\pi\pi$ three-channel model used here [28, 29]. The third threshold energy equal to 1.4 GeV is a parameter representing twice the mass of the effective two-pion mass $m_{(2\pi)}$ used to account for the four pion decays of scalar mesons (see Ref. [28]). Thus, in nature there is no such sharp energy behavior. These characteristic features of the pion scalar form factor $\Gamma_1^n(s)$ are essential to obtain a good fit of the experimental effective mass distributions of the $B^\pm$ to 3π decays.

The results of the fit on the experimental distributions, obtained using the NLO coefficients a_i^p in the $B^\pm \to \pi^\pm\pi^\mp\pi^\pm$ amplitudes, are displayed in Figs. 2, 3 and 4. The $\rho(770)$-resonance contribution dominates the $\pi^+\pi^-$ spectrum, but that of the S-wave is non negligible. As seen, the S-wave part is sizable near 500 MeV which is related to the contribution of the scalar resonance $f_0(600)$. Near 1.4 GeV the $f_0(1400)$ scalar resonance [28, 29] gives some enhancement in the distributions.

Figure 2 exhibits a small CP asymmetry, the B^- and B^+ effective mass distributions being very close. Summing the number of experimental events in the $m_{\pi^+\pi^-}$ range between 290 and 1640 MeV one finds 616 events for the B^- decay and 606 for that of the B^+. This leads to a CP asymmetry of $(0.8 \pm 4.8)\%$ which can be compared to the values of $(3.0 \pm 0.4)\%$ for the NLO fit and $(0.07 \pm 0.03)\%$ for the LO fit. Taking into account the statistical error of 4.8% and adding to it a few percent systematic error one sees that both fits agree with experiment. Let us recall here the experimental value of the CP asymmetry $A_{CP} = \left(3.2 \pm 4.4 \pm 3.1^{+2.5}_{-2.0}\right)\%$ for the total sample of $\pi^\pm\pi^\mp\pi^\pm$ events [5]. For the particular decay mode, namely for the $B^\pm$ decay into $\rho^0(770)\pi^\pm$, $\rho^0(770) \to \pi^+\pi^-$, the isobar model analysis gives $A_{CP} = \left(18 \pm 7 \pm 5^{+2}_{-14}\right)\%$, while from our model we get 4.4% (−0.03%). Note here that the asymmetries obtained for the fit corresponding to

the amplitudes calculated with the real LO a_i^p coefficients are quite small as it could have been expected.

Figures 3 and 4 show a spectacular feature, namely that the interference term of the S and P waves is quite important even at the $\rho(770)^0$ maximum. The sign of this interference term depends on the sign of $\cos\theta$, so the ρ peak is reduced for the negative values of $\cos\theta$ and enhanced for the positive values. This is a clear indication that the $\pi^+\pi^-$ effective mass distribution cannot be reproduced without the S-wave contribution. The $f_0(980)$ resonance is not observed as a peak in the $\pi^+\pi^-$ spectrum. This fact is easily explained in our model since the decay amplitudes are proportional to the pion scalar form factor which has a dip near 1 GeV as seen in Fig. 1. One can notice some surplus of events in the $\pi^+\pi^-$effective mass close to 1.25 GeV. In the isobar model analysis this was taken in account by introducing the $f_2(1270)$ resonance [5]. In the QCD factorization model applied here tensor mesons cannot be generated by the presently existing transition operators.

VI. SUMMARY AND OUTLOOK

The present paper is a continuation of our efforts [1–4] in constraining theoretically the meson-meson final state strong interactions in hadronic charmless three-body B decays. If the strong interaction amplitudes are sufficiently well understood then one can improve the precision of the weak interaction amplitudes extracted from these reactions.

Our theoretical model for the $B^\pm \to \pi^\pm\pi^\mp\pi^\pm$ is based on the application of the QCD factorization [6, 7, 9, 13] to quasi two-body processes in which only two of the three produced pions interact strongly, forming either an S- or P-wave state. One assumes that the third pion, being fast in the B-meson decay frame, does not interact with this pair. This hypothesis is mainly valid in a limited range of the $\pi^+\pi^-$ effective mass, here taken between the $\pi\pi$ threshold and 1.64 GeV.

The short-distance interaction part of the decay amplitudes describes the flavor changing processes $b \to u\bar{u}d$ and $b \to d\bar{d}d$. It is proportional to Cabibbo-Kobayashi-Maskawa matrix elements multiplied by effective coefficients calculable in the perturbative QCD formalism. This short-distance amplitude is multiplied by a long-distance contribution expressed in terms of two products. The first one is the product of the pion decay constant by the $B \to \pi\pi$ transition matrix element and the second one is the product of the pion form factor by the $B \to \pi$ transition form factor. The parametrization [Eqs. (16), (17)] of the scalar and vector B to π transition form factors follow from the light-cone sum rule study of Ref. [21].

The effective Wilson coefficients are calculated to next-to-leading order in the strong coupling constant. They include vertex and penguin corrections but neither hard-scattering ones nor annihilation contributions since these last two terms contain unknown phenomenological parameters related to amplitude divergences [9]. We find that these vertex and penguin corrections are small in comparison to the leading order term (see Table I). However, they allow to generate some non-zero CP asymmetries.

We then assume the B to $\pi\pi$ transition matrix element to be equal to the product of the B to intermediate meson transition form factor by the decay amplitude of this meson into two pions. The next step is to suppose the latter decay amplitude to be proportional to the pion non-strange scalar or vector form factor depending on the wave studied. For the S wave the proportionality factor is given by a fitted parameter χ_S and for the P wave it is related to the inverse of the ρ decay constant. For the limited range of the effective $\pi\pi$ mass, from $\pi\pi$ threshold to 1.64 GeV, the $B \to \pi\pi$ transition form factors are taken as constants given by the $B \to f_0(980)$ [19] and by the $B \to \rho(770)$ [20] transition form factors at $q^2 = m_\pi^2$.

The pion scalar form factor is modeled by the unitary relativistic three coupled-channel equation (24) using the $\pi\pi$, $K\bar{K}$ and effective $(2\pi)(2\pi)$ scattering T matrix of Refs. [28, 29]. This form factor depends on two fitted parameters: the first one κ insures the convergence of the involved integrals and the second one, c, controls the high-energy behavior of the production functions accountable for the meson pair formation. The pion vector form factor takes into account the contribution of the $\rho(770)$, $\rho(1450)$ and $\rho(1700)$, and follows from the parametrization of the Belle Collaboration in their study of the semi-leptonic $\tau^- \to \pi^-\pi^0\nu_\tau$ decays. For the P-wave amplitude we introduce a fitted overall normalization factor N_P.

We obtain a good fit to the $\pi\pi$ effective mass distributions of the BABAR Collaboration data of the $B^\pm \to \pi^\pm\pi^\mp\pi^\pm$ decays [5]. The value of the branching fraction for the $B^\pm \to \rho(770)^0\pi^\pm$ decays, $(8.2 \pm 0.5\times)10^{-6}$, agrees well with that, $(8.1 \pm 0.7 \pm 1.2^{+0.4}_{-1.1}) \times 10^{-6}$, of the experimental analysis. We find the normalization factor N_P to be close to 1. The $\pi^+\pi^-$ spectra are dominated by the $\rho(770)^0$ resonance but, at low effective mass, the S-wave contribution is sizable. Here the $f_0(600)$ resonance manifests its presence. Furthermore one observes a strong interference of the S and P waves in the event distributions for $\cos\theta > 0$ and $\cos\theta < 0$. Here the $f_0(980)$ is not directly visible as a peak, since the pion scalar form factor has a dip near 1 GeV. At 1.4 GeV, the maximum of the S-wave distribution comes from the scalar resonance $f_0(1400)$ [28, 29].

Our model yields a unified description of the contribution of the three scalar resonances $f_0(600)$, $f_0(980)$ and $f_0(1400)$ in terms of one function: the pion non-strange scalar form factor. This reduces

strongly the number of needed free parameters to analyze the Dalitz plot. The functional form of our S-wave amplitude [Eq. (20)], proportional to $\Gamma_1^{n*}(s)$, could be used in Dalitz-plot analyses and the table of $\Gamma_1^{n*}(s)$ values can be sent upon request.

The strong interaction phases of the decay amplitudes are constrained by unitarity and meson-meson data, which should help in the extraction of the weak angle phase γ or ϕ_3 equals to $\arg(-\lambda_u^*/\lambda_c^*)$. Of course new experimental data with better statistics would be welcome. One expects $B^\pm \to \pi^\pm\pi^\mp\pi^\pm$ events from the Belle Collaboration, and probably, in the near future, from LHCb and from the near term super B factories.

Acknowledgments

The authors are obliged to Bachir Moussallam for providing them the values of his pion scalar form factor $\Gamma_1^n(s)$ and to Gagan Bihari Mohanty for useful comments on the BABAR data. We are very grateful to Maria Różańska, Bachir Moussallam, Eli Ben-Haim and José Ocariz for helpful discussions. This work has been supported in part by the Polish Ministry of Science and Higher Education (grant No N N202 248135) and by the IN2P3-Polish Laboratories Convention (project No 08-127).

Appendix A: Long-distance functions $X_{S,P}$ and $Y_{S,P}$

1. The function X_S from the S-wave amplitude proportional to BR_S transition matrix element

From Eq. (12) the function X_S reads

$$\begin{aligned} X_S &\equiv \left\langle [\pi^+(p_2)\pi^-(p_3)]_S|(\bar{u}b)_{V-A}|B^-\right\rangle \left\langle \pi^-|(\bar{d}u)_{V-A}|0\right\rangle \\ &= G^n_{R_S\pi^+\pi^-}(s_{23})\left\langle R_S|(\bar{u}b)_{V-A}|B^-\right\rangle \left\langle \pi^-|(\bar{d}u)_{V-A}|0\right\rangle, \end{aligned} \tag{A1}$$

where the vertex function $G^n_{R_S\pi^+\pi^-}(s_{23})$ describes the R_S decay into a $[\pi^+\pi^-]_S$ pair. The B to R_S transition matrix element reads (see e.g. Eq. (B6) of Ref. [12])

$$\begin{aligned} &\langle R_S(p_2+p_3)|\bar{u}\gamma^\mu(1-\gamma^5)b|B^-(p_B)\rangle \\ &\qquad = i\left\{ \left[(p_B+p_2+p_3)^\mu - \frac{M_B^2-s_{23}}{m_\pi^2}p_1^\mu\right] F_1^{BR_S}(m_\pi^2) + \frac{M_B^2-s_{23}}{m_\pi^2}p_1^\mu F_0^{BR_S}(m_\pi^2)\right\}, \end{aligned} \tag{A2}$$

where $F_0^{BR_S}(m_\pi^2)$ and $F_1^{BR_S}(m_\pi^2)$ are the BR_S scalar and vector form factors, respectively. The pion decay constant f_π is defined as

$$\langle \pi^-(p_1)|\bar{d}\gamma_\mu(1-\gamma_5)u|0\rangle = if_\pi p_{1\mu}. \tag{A3}$$

The product of Eqs. (A2) and (A3) yields

$$\left\langle R_S|(\bar{u}b)_{V-A}|B^-\right\rangle \left\langle \pi^-|(\bar{d}u)_{V-A}|0\right\rangle = -(M_B^2 - s_{23})f_\pi F_0^{BR_S}(m_\pi^2). \tag{A4}$$

The vertex function $G^n_{R_S\pi^+\pi^-}(s_{23})$, as in Ref. [2], is modeled by

$$\left\langle [\pi^+\pi^-]_S|\bar{n}n|0\right\rangle = G^n_{R_S\pi^+\pi^-}(s_{23})\left\langle R_S|\bar{n}n|0\right\rangle. \tag{A5}$$

An effective scalar decay constant $f^n_{R_S}$ can be introduced with

$$\langle R_S|\bar{n}n|0\rangle = m_{R_S}\, f^n_{R_S}. \tag{A6}$$

From Eqs. (A5), (18) and (A6) one obtains

$$G^n_{R_S\pi^+\pi^-}(s_{23}) = \sqrt{\frac{2}{3}}\,\chi_S\,\Gamma_1^{n*}(s_{23}) = \sqrt{\frac{2}{3}}\,\frac{\sqrt{2}B_0}{m_{R_S}\, f^n_{R_S}}\Gamma_1^{n*}(s_{23}), \tag{A7}$$

with

$$\chi_S = \frac{\sqrt{2}B_0}{m_{R_S}\, f^n_{R_S}}. \tag{A8}$$

The effective scalar decay constant has a role comparable to the R_P decay constant as can be seen comparing Eqs. (A7) and (A19). The product of Eqs. (A7), (A2) and (A3) gives

$$X_S = -\sqrt{\frac{2}{3}}\,\chi_S\, f_\pi\,(M_B^2 - s_{23})\,F_0^{BR_S}(m_\pi^2)\,\Gamma_1^{n*}(s_{23}). \tag{A9}$$

2. The function Y_S from the S-wave amplitude proportional to $B\pi$ transition matrix element

From Eq. (13) one has

$$\begin{aligned} Y_S &\equiv \left\langle \pi^-|(\bar{d}b)_{sc-ps}|B^-\right\rangle \left\langle [\pi^+(p_2)\pi^-(p_3)]_S|(\bar{d}d)_{sc+ps}|0\right\rangle \\ &= \left\langle \pi^-|\bar{d}b|B^-\right\rangle \left\langle [\pi^+(p_2)\pi^-(p_3)]_S|\bar{d}d|0\right\rangle. \end{aligned} \tag{A10}$$

From the Dirac equations satisfied by $b(p_B)$ and $\bar{d}(p_1)$ one obtains

$$\left\langle \pi^-(p_1)\left|\bar{d}(p_1)b(p_B)\right|B^-(p_B)\right\rangle = \left\langle \pi^-(p_1)\left|\bar{d}(p_1)\frac{\gamma\cdot(p_B-p_1)}{m_b-m_d}b(p_B)\right|B^-(p_B)\right\rangle . \tag{A11}$$

The B to π transition matrix element $\left\langle \pi^-|(\bar{d}b)_{V-A}|B^-\right\rangle$, entering into the above expression, can be written as (see e.g. Eq. (5) of Ref. [3])

$$\begin{aligned}&\langle \pi^-(p_1)|\bar{d}\gamma^\mu(1-\gamma^5)b|B^-(p_B)\rangle \\ &\qquad = \left[(p_B+p_1)^\mu - \frac{M_B^2-m_\pi^2}{q^2}q^\mu\right]F_1^{B\pi}(q^2) + \frac{M_B^2-m_\pi^2}{q^2}q^\mu F_0^{B\pi}(q^2),\end{aligned} \tag{A12}$$

where $F_0^{B\pi}(q^2)$ and $F_1^{B\pi}(q^2)$ are the $B\pi$ scalar and vector form factors, respectively and $q = p_B - p_1 = p_2 + p_3$. Using Eqs. (A12) and (18) in Eq. (A10), yields

$$Y_S = \sqrt{\frac{2}{3}}\, B_0\, \Gamma_1^{n*}(s_{23})\, \frac{M_B^2-m_\pi^2}{m_b-m_d}\, F_0^{B\pi}(s_{23}). \tag{A13}$$

3. The function X_P from the P-wave amplitude proportional to BR_P transition matrix element

From Eq. (14) one has for the function X_P (see Eq. (3.1) of Ref. [12])

$$\begin{aligned}X_P &\equiv \left\langle [\pi^+(p_2)\pi^-(p_3)]_P|(\bar{u}b)_{V-A}|B^-\right\rangle \left\langle \pi^-|(\bar{d}u)_{V-A}|0\right\rangle \\ &= \frac{G^n_{R_P\pi^+\pi^-}(s_{23})}{\sqrt{2}}\,\epsilon\cdot(p_2-p_3)\left\langle R_P|(\bar{u}b)_{V-A}|B^-\right\rangle \left\langle \pi^-|(\bar{d}u)_{V-A}|0\right\rangle ,\end{aligned} \tag{A14}$$

where the R_P decay into a $[\pi^+\pi^-]_P$ pair is described by the vertex function $G^n_{R_P\pi^+\pi^-}(s_{23})$. Here ϵ represents the polarization vector of the P-wave meson R_P. The factor $1/\sqrt{2}$ comes from the fact that R_P represents the $\rho(770)^0$. As seen from e.g. Eq. (B6) of Ref. [12] or Eq. (24) of Ref. [6],

$$\left\langle R_P(p_2+p_3)|(\bar{u}b)_{V-A}|B^-(p_B)\right\rangle = -i\,2m_{R_P}\,\frac{\epsilon^*\cdot p_B}{p_1^2}\,p_1\,A_0^{BR_P}(p_1^2) + \text{other terms}. \tag{A15}$$

The "other terms" do not give any contribution when multiplying this matrix element by that given in Eq. (A3). Plugging this expression into Eq. (A14) one has a product of polarization vectors and the sum over the three possible polarization eigenvalues of the state R_P should be done. From

$$\sum_{\lambda=0,\pm1}\epsilon_\mu^\lambda(p)\epsilon_\nu^{\lambda*}(p) = -(g_{\mu\nu} - \frac{p_\mu p_\nu}{p^2}), \tag{A16}$$

one obtains

$$\sum_{\lambda=0,\pm1} \epsilon^{\lambda} \cdot (p_2 - p_3)\epsilon^{\lambda^*} \cdot p_B = -p_1 \cdot (p_2 - p_3). \tag{A17}$$

Then

$$X_P = \frac{f_\pi}{f_{R_P}} F_1^{\pi\pi}(s_{23})\ (s_{13} - s_{12})\ A_0^{BR_P}(m_\pi^2). \tag{A18}$$

Above, as shown in Ref. [3] for the $K^*(892) \to (K\pi)_P$ decay case [see their Eq. (D9)], we have parametrized the $R_P\pi^+\pi^-$ vertex function in terms of the pion vector form factor $F_1^{\pi\pi}(s_{23})$. One has

$$G_{R_P\pi^+\pi^-}(s_{23}) = \frac{\sqrt{2}}{m_{R_P} f_{R_P}} F_1^{\pi\pi}(s_{23}), \tag{A19}$$

f_{R_P} being the charged R_P decay constant.

4. The function Y_P from the P-wave amplitude proportional to the $B\pi$ transition matrix element

From Eq. (15)

$$Y_P \equiv \left\langle \pi^-|(\bar{d}b)_{V-A}|B^-\right\rangle \ \left\langle [\pi^+(p_2)\pi^-(p_3)]_P|(\bar{u}u)_{V-A}|0\right\rangle . \tag{A20}$$

The pion vector form factor is defined by (see e.g. Eq. (36) of Ref. [6])

$$\langle R_P|(\bar{u}u)_{V-A}|0\rangle = \langle [\pi^+(p_2)\pi^-(p_3)]_P|\bar{u}\gamma_\mu(1-\gamma^5)u|0\rangle = -\left(p_2 - p_3\right)_\mu F_1^{\pi\pi}(q^2). \tag{A21}$$

The minus sign arises from the definition of the form factor $F_1^{\pi\pi}(q^2)$ which contains a plus sign for a $(\bar{d}d)_{V-A}$ current [similar to Eq. (A12], then as $\rho^0 = 1/\sqrt{2}(u\bar{u} - d\bar{d})$, there will be a minus sign for a $(\bar{u}u)_{V-A}$ current. The product of Eqs. (A12) and (A21) gives

$$Y_P = -2\, p_1 \cdot (p_2 - p_3)\, F_1^{B\pi}(q^2) F_1^{\pi\pi}(q^2) = (s_{13} - s_{12}) F_1^{B\pi}(q^2) F_1^{\pi\pi}(q^2). \tag{A22}$$

Appendix B: Linear system of equations for α_i^n, τ_i^n and ω_i^n

The linear system of nine equations satisfied by the nine production function parameters α_i^n, τ_i^n and ω_i^n, $i = 1, 2, 3$, is

$$
\begin{aligned}
\alpha_i^n + \sum_{j=1}^{3} \alpha_j^n H_{ji}(0) &= d_i^n, \\
\tau_i^n + \sum_{j=1}^{3} \left(\tau_j^n H_{ji}(0) + \alpha_j^n \frac{\partial H_{ji}(E)}{\partial E}\bigg|_{E=0} \right) &= 0, \\
\omega_i^n + \sum_{j=1}^{3} \left(\omega_j^n H_{ji}(0) + \tau_j^n \frac{\partial H_{ji}(E)}{\partial E}\bigg|_{E=0} + \frac{1}{2}\alpha_j^n \frac{\partial^2 H_{ji}(E)}{\partial E^2}\bigg|_{E=0} \right) &= f_i^n. \qquad \text{(B1)}
\end{aligned}
$$

[1] A. Furman, R. Kamiński, L. Leśniak and B. Loiseau, Phys. Lett. B **622**, 207 (2005), *Long-distance effects and final state interactions in $B \to \pi\pi K$ and $B \to K\bar{K}K$ decays.*

[2] B. El-Bennich, A. Furman, R. Kamiński, L. Leśniak and B. Loiseau, Phys. Rev. D **74**, 114009 (2006), *Interference between $f_0(980)$ and $\rho(770)^0$ resonances in $B \to \pi^+\pi^-K$ decays.*

[3] B. El-Bennich, A. Furman, R. Kamiński, L. Leśniak, B. Loiseau, B. Moussallam, Phys. Rev. D **79**, 094005 (2009), *CP violation and kaon-pion interactions in $B \to K\pi^+\pi^-$ decays.*

[4] O. Leitner, J.-P. Dedonder, B. Loiseau, and R. Kaminski, Phys. Rev. D **81**, 094033 (2010), *K^* resonance effects on direct CP violation in $B \to \pi\pi K$.*

[5] B. Aubert, *et al.* (BABAR Collaboration), Phys. Rev. D **79**, 072006 (2009), *Dalitz-plot analysis of $B^\pm \to \pi^\pm\pi^\mp\pi^\pm$ decays.*

[6] A. Ali, G. Kramer and Cai-Dian Lü, Phys. Rev. D **58**, 094009 (1998), *Experimental tests of factorization in charmless nonleptonic two-body B decays.*

[7] M. Beneke, G. Buchalla, M. Neubert and C. T. Sachrajda, Nucl. Phys. **B606**, 245 (2001), *QCD factorization in $B \to \pi K, \pi\pi$ decays and extraction of Wolfenstein parameters.*

[8] S. Gardner and U.-G. Meißner, Phys. Rev. D **65**, 094004 (2002), *Rescattering and chiral dynamics in $B \to \rho\pi$ decays.*

[9] M. Beneke and M. Neubert, Nucl. Phys. **B675**, 333 (2003), *QCD factorization for $B \to PP$ and $B \to PV$ decays.*

[10] O. Leitner, X-H. Guo, A.W. Thomas, J. Phys. G: Nucl. Part. Phys. **31**, 199 (2005), *Direct CP violation, branching ratios and form factors $B \to \pi$, $B \to K$ in B decays.*

[11] H. Y. Cheng, C. K. Chua and K. C. Yang, Phys. Rev. D **73**, 014017 (2006), *Charmless hadronic B decays involving scalar mesons: implications to the nature of light scalar mesons.*

[12] H-Y. Cheng, C-K. Chua and A. Soni, Phys. Rev D **76**, 094006 (2007), *Charmless three-body decays of B mesons.*

[13] M. Beneke, Nucl. Phys. B (Proc. Suppl.) **170**, 57 (2007), *Hadronic B decays.*

[14] A. Deandrea and A. D. Polosa, Phys. Rev. Lett. **86**, 216 (2001), *$B \to \rho\pi$ decays, Resonant and Nonresonant Contributions.*

[15] B. Aubert, *et al.* (BABAR Collaboration), Phys. Rev. D **76**, 012004 (2007), *Measurement of CP-violating asymmetries in $B^0 \to (\rho\pi)^0$ using a time-dependent Dalitz-plot analysis.*

[16] A. Kusaka, *et al.* (Belle Collaboration), Phys. Rev. D **77**, 072001 (2008), *Measurement of CP asymmetries and branching fractions in a time-dependent Dalitz-plot analysis of $B^0 \to (\rho\pi)^0$ and a constraint on the quark mixing angle ϕ_2.*

[17] M. Beneke in Three-Body Charmless B Decays Workshop, `http://lpnhe-babar.in2p3.fr/3BodyCharmlessWS/`, February 1-3, 2006, LPNHE, Paris, *Quasi two-body and three-body decays in the heavy quark expansion.*

[18] C. Amsler *et al.* (Particle Data Group), Phys. Lett. B **667**, 1 (2008), *Review of particle physics.*

[19] B. El-Bennich, O. Leitner, J.-P. Dedonder, B. Loiseau, Phys. Rev. D **79**, 076004 (2009), *The Scalar Meson $f_0(980)$ in Heavy-Meson Decays.*

[20] P. Ball, V. M. Braun, Phys. Rev. D **58**, 094016 (1998) [arXiv: hep-ph/9805422], *Exclusive semileptonic and rare B meson decays in QCD.*

[21] P. Ball and R. Zwicky Phys. Rev. D 71, 014015 (2005), *New results on $B \to \pi,\ K, \eta$ decay form factors from light-cone sum rules.*

[22] G. Barton, *Introduction to dispersion techniques in field theory*, Benjamin, New-York, 1965.

[23] H.-Y. Cheng, C. K. Chua and C. W. Hwang, Phys Rev. **D** 69, 074025 (2004), *Covariant light-front approach for S-wave and P-wave mesons: Its application to decay constants and form factors.*

[24] N. I. Muskhelishvili, Singular integral equations, (P.Nordhof 1953), chapters 18 and 19; R. Omnès, Nuovo Cim. **8**, 316 (1958), *On the Solution of certain singular integral equations of quantum field theory.*

[25] J. F. Donoghue, J. Gasser, H. Leutwyler, Nucl. Phys. **343**, 341 (1990), *The decay of a light Higgs boson.*

[26] B. Moussallam, Eur. Phys. J. C **14**, 111 (2000), *N_f dependence of the quark condensate from a chiral sum rule.*

[27] U.-G. Meißner and J. A. Oller, Nucl. Phys. **A679**, 671 (2001), *$J/Psi \to \phi\pi\pi(K\bar{K})$ decays, chiral dynamics and OZI violation.*

[28] R. Kamiński, L. Leśniak and B. Loiseau, Phys. Lett. B **413** (1997) 130, *Three channel model of meson meson scattering and scalar meson spectroscopy.*

[29] R. Kamiński, L. Leśniak and B. Loiseau, Eur. Phys. J. **C9**, 141 (1999), *Scalar mesons and multichannel amplitudes.*

[30] R. Kamiński and L. Leśniak, J.-P. Maillet, Phys. Rev. D **50**, 3145 (1994), *Relativistic effects in scalar meson dynamics.*

[31] Yoshio Yamaguchi and Yoriko Yamaguchi , Phys. Rev. **95**, 1635 (1954), *Two-Nucleon Problem When the Potential Is Nonlocal but Separable. II.*

[32] T. A. Lähde, and U.-G. Meißner, Phys. Rev. D **74**, 034021 (2006), *Improved analysis of J/ψ decays into a vector meson and two pseudoscalars.*

[33] C. Allton, *et al.* (RBC and UKQCD Collaborations), Phys. Rev. D **78**, 114509 (2008), *Physical results*

from $2+1$ *flavor domain wall QCD and SU(2) chiral perturbation theory.*

[34] M. Fujikawa *et al.* (Belle Collaboration), Phys. Rev. D **78**, 072006 (2008), *High-statistics study of the* $\tau^- \to \pi^-\pi^0\nu_\tau$ *decay.*

[35] P. Ball and G. W. Jones, JHEP 0703, 69 (2007), *Twist-3 distribution amplitudes of* K^* *and* ϕ *mesons.*

[36] B. Moussallam, private communication.